Письма в ЭЧАЯ. 2014. Т. 11, № 5(189). С. 1092–1098

ФИЗИКА И ТЕХНИКА УСКОРИТЕЛЕЙ

# DEVELOPMENT OF POSITRON ANNIHILATION SPECTROSCOPY AT LEPTA FACILITY

*P. Horodek* [a,b,1], *M. Bugdol* [c], *A. G. Kobets* [a,d], *I. N. Meshkov* [a], *O. S. Orlov* [a], *A. Yu. Rudakov* [a], *A. A. Sidorin* [a], *S. L. Yakovenko* [a]

[a] Joint Institute for Nuclear Research, Dubna
[b] Institute of Nuclear Physics, PAS, Cracow, Poland
[c] Institute of Physics, Opole University, Opole, Poland
[d] Institute of Electrophysics and Radiation Technologies, NAS of Ukraine, Kharkov, Ukraine

The Low Energy Positron Toroidal Accumulator (LEPTA) at JINR proposed for generation of positronium in flight can be used for Positron Annihilation Spectroscopy (PAS). This is the sensitive method for microstructure studies of solid body. The structural defects such as vacancies, vacancy clusters and nano-voids with the size of 0.1–10 nm can be detected. In this paper, the progress in the development of PAS at LEPTA facility is presented. The description of the Doppler broadening of annihilation gamma-line technique and the examples of results obtained on slow positron beam are shown.

Тороидальный накопитель позитронов низкой энергии (LEPTA) в ОИЯИ, предназначенный для генерации позитрония на лету, может быть использован для позитронной аннигиляционной спектроскопии (ПАС). Это чувствительный метод для изучения структуры твердого тела. Им могут быть обнаружены дефекты в структуре, такие как вакансии, кластеры вакансий и нанопустоты размерами 0,1–10 нм. Представлен ход развития ПАС на установке LEPTA. Также описан метод доплеровского уширения аннигиляционных линий и приведены примеры результатов, полученных на медленном позитронном пучке.

PACS: 29.30.Ep; 41.75.Fr; 61.72.jd

## INTRODUCTION

The aim of Positron Annihilation Spectroscopy (PAS) is detection of open-volume defects such as vacancies in solid-body lattice. Theoretically, a perfect structure in real world is never free from many kinds of imperfections, which influence the material properties. The application of PAS allows one to recognize the type of defect and determine its concentration. It is important especially in the case of points defects which are hard to be seen by other methods.

Due to the special properties of positron–electron annihilation process, observation of emitted gamma quanta via the Doppler Broadening of annihilation Gamma Line 511 keV (DBGL) or by measurements of positron LifeTimes (LT) gives information about the type and concentration of defects smaller than 10 nm. Using slow positron beam allows one to observe it at the depth of about 1 $\mu$m below the surface.

[1] E-mail: Pawel.Horodek@ifj.edu.pl

## THE DOPPLER BROADENING OF ANNIHILATION GAMMA LINE (DBGL)

The meeting of an electron ($e^-$) and its antiparticle — positron ($e^+$), causes the annihilation process, while the mass of a pair $e^+e^-$ is converted into the energy of electromagnetic field and gamma quanta are emitted. The annihilation process with random electron takes place after thermalization, when, as a result of interactions with matter, it reduces the energy to circa 25 meV. In 99.7% cases it is the annihilation process into two gamma quanta. The possibility of annihilation on three or more photons exists but with very small probability [1, 2].

In the laboratory system the energy of emitted radiation will be changed as a result of the Doppler effect according to the formula

$$E_\gamma \cong mc^2 \pm \sqrt{\frac{1}{2}\, mc^2\, E}, \tag{1}$$

where $m$ is an electron, $c$ — a speed of light, and $E$ is an electron energy. In this expression, binding energy $e^+e^-$ and positron momentum were omitted. In fact, the changing energy depends on the parallel component of momentum of the pair $e^+e^-$, where positron momentum is negligible. The Doppler effect causes the broadening of 511-keV line.

Positron can pass the places, where the density of electrons is changed. These places are such defects of structure as vacancies (atoms missing), and positron can be localized there. The electron momenta inside defects are smaller. Thus, the broadening of annihilation gamma line will also be smaller.

The observation of DBGL consists in registration of gamma quanta 511 keV using spectrometer including the HPGe detector, an amplifier, a multichannel analyzer, which collected energy spectrum from annihilation process and a computer. The energy resolution of detector working at LEPTA facility is 1.2 keV.

The spectroscopy of the Doppler broadening of annihilation gamma line is mainly used to detect vacancies and their clusters as well as their concentration. The annihilation of a trapped positron gives the broadening of 511-keV line, but relatively smaller than that, which will appear in the case of annihilation of a positron with electrons of atomic core or conduction electrons. To simplify, the more defected sample, the less broadened 511-keV line. The quantitative connection between these values describes the so-called trapping model [3].

The shape of annihilation line depends on many factors, which are the reason why the analysis of this line consists in determining the proportion of annihilations with low- and high-momentum electrons by the use of $S$ and $W$ parameters. Here, only description of $S$ parameter will appear.

The $S$ parameter is determined as a ratio of an area under the central part of annihilation line to the whole area under this line after subtraction of the background. Usually the value of $S$ parameter is about 0.5.

The area under the line is selected arbitrarily, but the range wherein it is calculated should be predetermined within the framework of given measurement series. It allows one to monitor the behaviour of $S$ parameter under the influence of the factor disturbing the structure, e.g., plastic deformation. This parameter is sensitive to the presence of defects and connected to their concentration. The bigger value of $S$ parameter, the bigger concentration of defects such as vacancies.

In Fig. 1, the annihilation lines of 511 keV for two kinds of stainless steel samples are presented. The black line represents the nondefected one. The grey line comes from the

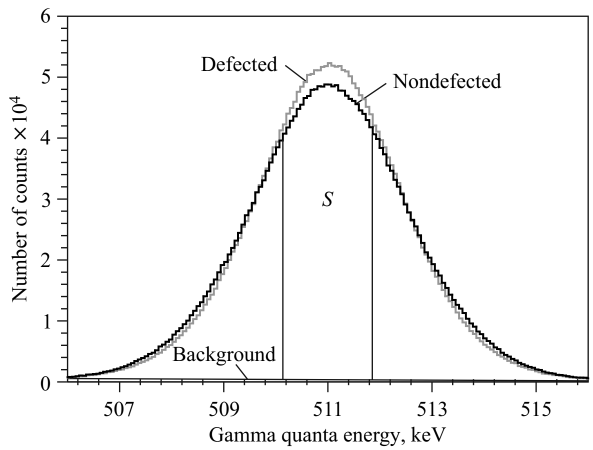


Fig. 1. The annihilation lines with marked areas defining $S$ parameter in stainless steel. The grey line comes from the defected (by sandblasting) sample, while the black one represents the nondefected sample

sample defected by sliding. The broadening in the case of the second specimen is much smaller. It points out that friction induces [4].

The experiment of the Doppler broadening of annihilation gamma line usually boils down to the calculation of this parameter. It allows one to conclude about defects concentration and their distribution.

## SLOW POSITRON BEAM AT LEPTA FACILITY

Since 2000, LEPTA (Low Energy Positron Torroidal Accumulator) project has been developing at the Joint Institute for Nuclear Research in Dubna. The main goal of this idea is to create an intense orthopositronium flux in flight. A positron injector in this project is a low positron beam, which can be used in PAS application [5].

The method of positron flux formation is following. Positrons after emission from $^{22}$Na source with 25 mCi being under potential $+50$ V go through the solid neon gas. It plays a role of a moderator causing the wide part of positrons at elastic scatterings to slow down to thermal speeds.

The cryogenic source dedicated to experiments is closed in a special stand, which includes neon and liquid helium lines. The $^{22}$Na isotope is placed in the vacuum chamber under the pressure of $4 \cdot 10^{-9}$ Torr. The liquid helium guarantees low temperature of about 7 K. Second line delivers neon, which creates condensed layer of moderator without cloud. In this way, the count intensity of the obtained flux is $3 \cdot 10^5$ s$^{-1}$ and the average energy equals 1.2 eV.

Next, the separation of slow and fast positrons is done by the use of 100 Gs magnetic field for transport of continuous beam of slow positrons. Slow positrons follow «slalom» trajectory, while the fast ones hit the aperture diafragma.

The negative potential applied to the sample allows one to accelerate positrons up to the initial energy of 35 keV. In this way, monoenergetic positrons are implanted into the sample.

## THE EXAMPLES OF APPLICATIONS

The first studies were performed for sample of pure copper annealed for 2 h at $900\,^\circ$C. The aim of this investigation was the application of our slow positron beam working at LEPTA facility for the specimen, which is well described in the literature. We wanted to compare the obtained results with those from the literature [6].

The measured $S$ parameter profile versus energy of implanted positrons is presented in Fig. 2. It decreases with positron energy and saturates for the energy of about 30 keV. This is the expected dependence. The solid black line represents the best fit of the so-called diffusion equation for our profile obtained using VEPFIT program [7]. The diffusion equation is presented below:

$$S(E) = S_{\text{zone}} + (S_{\text{surface}} - S_{\text{zone}}) \int\limits_0^\infty P(z, E) \exp\left(-\frac{z}{L_+}\right) dz, \tag{2}$$

where

$$P(z, E) = \frac{m z^{m-1}}{z_0^m} \exp\left[-\left(\frac{z}{z_0}\right)^m\right] \tag{3}$$

is the implantation profile for slow positrons

$$z_0(E) = \frac{A}{\rho \Gamma(1 + 1/m)} E^n, \tag{4}$$

and $E$ is the positron energy in keV. For copper we used the following parameters: $\rho = 8.96\ \text{g}\cdot\text{cm}^{-3}$, $A = 3.78 \cdot 10^{-6}\ \text{g}\cdot\text{cm}^{-2}\cdot\text{keV}^n$, $m = 1.78$, $n = 1.61$, and $\Gamma$ is a gamma function, thus $z_0 = 471E\ (\text{keV})^{1.61}$ [8]. $S_{\text{zone}}$ and $S_{\text{surface}}$ are the values of $S$ parameter for positrons annihilating only in the zone or at the surface, respectively. $L_+$ is the positron diffusion length

$$L_+ = \sqrt{\frac{D_+ \tau_{\text{bulk}}}{1 + \tau_{\text{bulk}}\, \mu C}}, \tag{5}$$

where $C$ is the defect concentration in the zone, $D_+$ — the positron diffusion coefficient, and $\mu$ is the positron-trapping coefficient in this defect. $L_+$ will be shorter for positrons annihilating in the defect in comparison to $L_+$ for nondefected sample.

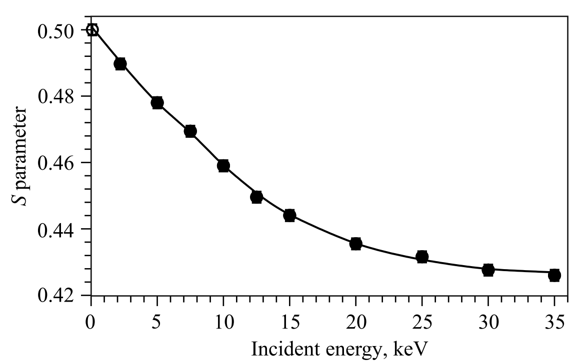


Fig. 2. The dependence of the measured $S$ parameter on the positron energy for the sample of pure Cu. The solid line represents the best fit of model curves obtained from VEPFIT [7]

Using VEPFIT program [7] to fit model function for the obtained results, the diffusion length equal to $(141 \pm 11)$ nm was obtained. It corresponds well with the value from the literature, where this quantity was 120–130 nm [6, 9]. It means that our experiment was perfomed correctly.

In the second investigations we tested the defected layer of samples of stainless steel grade 304 AISI annealed for 1 h at 700 °C in the flow $N_2$ atmosphere and next sandblasted under different pressures of 1, 3, 5 and 7 bar. The $N_2$ atmosphere is usually applied for protection materials for oxidation. The sandblasting is the surface treatment process used for removing oxide layer [10]. The results of DBGL are presented in Fig. 3, $a$.

The measured $S$ parameter profiles point out to the existence of at least two layers in the studied area equal to 1.3 $\mu$m. The estimation of the mean range of positron penetration was calculated as follows:

$$\bar{z} = \frac{A_{1/2}}{\rho} E^n, \tag{6}$$

where $\rho = 7.8 \text{ g} \cdot \text{cm}^{-3}$ is the density of material; $A_{1/2} = 2.39$ nm/keV$^n$ and $n = 1.692$ are the Makhov parameters for Fe [11]. For the reference sample (black circles), which represents only annealed sample, the similarity between the profile presented here and that obtained by Wu et al. [12] occurs. This profile lies under profiles of the sandblasted ones. It means that this sample was mostly defected. Additionally, we can observe ranges where decreasing $S$ parameter has different slopes. Between energies of 2 and 15 keV, it decreases linearly. At energy of 16 keV, there is another drop of a different kind, which seems to saturate at energies unavailable in this experiment. In the case of sandblasted specimens (white circles), we can recognize also two regions. In the first region, the saturation of $S$ parameter is visible. The layered character of the obtained profiles can be explained as the existence of oxide

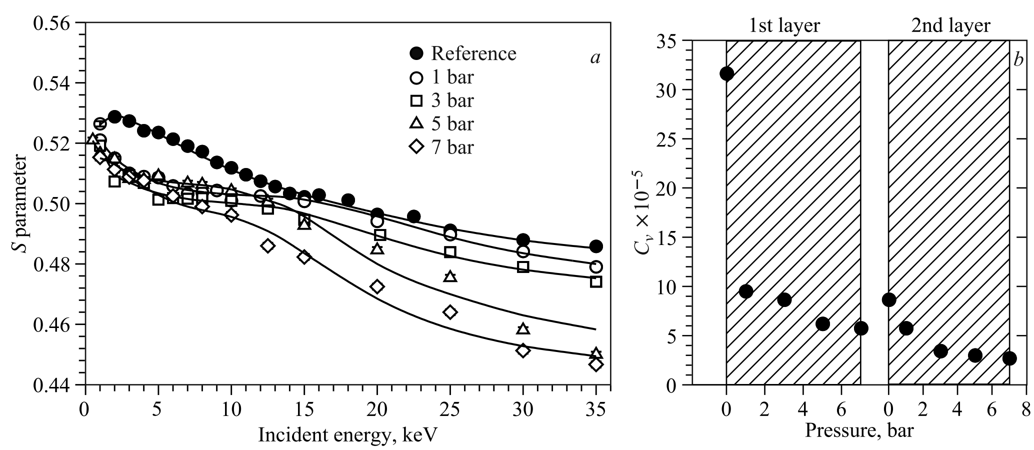


Fig. 3. $a$) The dependence of the measured $S$ parameter on the positron energy for the reference sample (black circles) and the sandblasted ones under pressures of 1 bar (white circles), 3 bar (white squares), 5 bar (white triangles) and 7 bar (white diamonds). The solid lines represent the best fit of model curves obtained from VEPFIT [7]. $b$) The dependence of vacancy concentration obtained using in two layers of sandblasted samples under pressures of 1, 3, 5, 7 bar. The value of 0 bar on $x$-axis represents the reference, nonsandblasted sample

layers on the surface. The stainless steel consists of elements as Fe, Ni and Cr, which can connect with oxide. Unfortunately, we cannot recognize which one it is. Additionally, we observed the reduction of the thickness of the first layer in dependency on pressure applied during sandblasting. Using VEPFIT program, the model function was fitted to the obtained results. It is marked by solid black line in Fig. 3, *a*. It allows one to approximate the thickness of the first layer. For the reference sample it is 337 nm, 207 nm — for sample sandblasted under the pressure of 1 bar, and 120 nm — for 7 bar. Additionally, the diffusion lengths made possible the approximation of defects concentration according to the formula

$$C = \frac{(L_{\rm bulk}/L_+)^2 - 1}{\tau_{\rm bulk}\,\mu}, \tag{7}$$

where $t_{\rm bulk} = 109.6$ ps [13], $\mu$ is the trapping coefficient for a single vacancy in pure Fe equal to $1.1 \cdot 10^{15}$ s$^{-1}$ [14], $L_{\rm bulk} = 142$ nm [15] (the positron diffusion length in the bulk). The defects concentration, which we recognized as vacancies, decreses in two layers in dependency on pressure, applied during sandblasting. It is visible in Fig. 3, *b*. For the reference sample (0 bar in Fig. 3, *b*), the vacancy concentration was $3.16 \cdot 10^{-4}$ in the first layer and $8.64 \cdot 10^{-5}$ in the second one. In the case of sample sandblasted under 7 bar, it was $8.64 \cdot 10^{-5}$ and $2.68 \cdot 10^{-5}$, respectively. The values were given in relative units, it means a number of defects per a number of atoms in the lattice. Sandblasting does not introduce defects into the sample, as we could expect, but reduces its presence in the studied area.

## SUMMARY

The PAS offers possibilities of detection of structural defects in the materials. Using slow positron beams allows one to investigate changes in the lattice close to the surface. The positron flux developed at LEPTA facility seems to be appropriate to these investigations. Tests performed on this beam confirm it. The example of applications shows that DBGL measurements can point out to the interesting properties of the surface zone.

The nearest plans concerning slow positron beam at LEPTA facility will focus on the studies of materials defected in many ways, e.g., surface treatment, radiation damages or ion implantation. Additionally, we are going to reorganize present continuous beam into the so-called pulsed positron beam. The creation of short pulses no longer than 100 ps allows for positron lifetime measurements. As a result, apart from information about defects concentration, the determination of the kind of defect will be possible.

All works were supported by RFBR grant No. 12-02-00072.

## REFERENCES

1. *Brandt W., Dupasquier A.* // Proc. of Intern. School of Physics Enrico Fermi: Positrons Solid-State Physics, Course LXXXIII, Varenna, 1981. Amsterdam, 1983.
2. *Dupasquier A., Mills A. P., Jr.* // Proc. of Intern. School of Physics Enrico Fermi: Positron Spectroscopy of Solids, Course CXXV, Varenna, 1993. Amsterdam, 1995.
3. *Frieze W. E., Lynn K. G., Welch D. O.* Positron Trapping Model Including Spatial Diffusion of the Positron // Phys. Rev. B. 1985. V. 31. P. 15–19.

4. *Horodek P. et al.* // Proc. of RUPAC2012, Positron Annihilation Spectroscopy at LEPTA Facility; http://accelconf.web.cern.ch/AccelConf/rupac2012/papers/weppc044.pdf.
5. *Akhmanova E. V. et al.* LEPTA Project: Formation and Injection of Positron Beam // Phys. Part. Nucl. Lett. 2012. V. 9. P. 373–376.
6. *Dryzek J. et al.* Subsurface Zones Created under Lubrication Conditions Studied by Positron Annihilation // Tribol. Lett. 2001. V. 11. P. 29–36.
7. *Van Veen A., Schut H., Clement M.* VEPFIT Applied to Depth Profiling Problems // Appl. Surf. Sci. 1995. V. 85. P. 216–224.
8. *Aers G. C., Jensen K. O., Walker A. B.* Slow Positron Beam Techniques for Solids and Surfaces // AIP Conf. Proc. V. 303. New York: AIP Press, 1994. P. 13.
9. *Britton D. T. et al.* Positron Reflection from the Surface Potential // Phys. Rev. Lett. 1989. V. 62. P. 2413.
10. *Lindell D., Pettersson R.* Pickling of Process-Oxidized Austenitic Stainless Steels in HNNO3-HF Mixed Acid // Steel Res. Int. 2010. V. 81, Iss. 7. P. 542–551.
11. *Dryzek J., Horodek P.* GEANT4 Simulation of Slow Positron Beam Implantation Profiles // Nucl. Instr. Meth. B. 2008. V. 266.
12. *Wu Y. C. et al.* Slow Positron Beam Study of Corrosion — Related Defects in Pure Iron // Appl. Surf. Sci. 2006. V. 252. P. 3274.
13. *Horodek P., Dryzek J., Wróbel M.* Positron Annihilation Study of Defects Induced by Various Cutting Methods in Stainless Steel Grade 304 // Tribol. Lett. 2012. V. 45. P. 341–347.
14. *Vehanen A. et al.* Vacancies and Carbon Impurities in A-Iron: Electron Irradiation // Phys. Rev. B. 1982. V. 25. P. 762–780.
15. *Lukáč F. et al.* Vacancy-Induced Hardening in Fe–Al Alloys // J. Phys. Conf. Ser. 2013. V. 443. P. 012025.